

Charged hadron fragmentation functions at high energy colliders

Ignacio Borsa^{*} and Marco Stratmann[†]

*Institute for Theoretical Physics, University of Tübingen,
Auf der Morgenstelle 14, 72076 Tübingen, Germany*

Daniel de Florian[‡]

*International Center for Advanced Studies (ICAS) and IFICI, UNSAM,
Campus Miguelete, 25 de Mayo y Francia (1650) Buenos Aires, Argentina*

Rodolfo Sassot[§]

*Universidad de Buenos Aires, Facultad de Ciencias Exactas y Naturales,
Departamento de Física and IFIBA-CONICET, Ciudad Universitaria, (1428) Buenos Aires, Argentina*

 (Received 30 November 2023; accepted 28 February 2024; published 14 March 2024)

We update our extraction of parton-to-charged hadron fragmentation functions at next-to-leading order accuracy in quantum chromodynamics (QCD), focusing on the wealth of data collected at the Large Hadron Collider over the past decade. We obtain an accurate description of single-inclusive processes involving unidentified charged hadrons produced at different rapidities and transverse momenta in proton-proton collisions in a wide range of center-of-mass system energies between 0.9 and 13 TeV, along with measurements performed in proton-antiproton collisions at the Tevatron Collider in the past. Next-to-leading order estimates of charged hadron production rates agree best with data when the theoretical factorization scales are selected similar to those optimized for identified pions, kaons, and protons in a recent global QCD analysis.

DOI: [10.1103/PhysRevD.109.052004](https://doi.org/10.1103/PhysRevD.109.052004)

I. INTRODUCTION

The production of charged hadrons with large transverse momentum p_T in hadronic collisions is an ubiquitous tool used to explore different aspects of the structure of matter, its constituents, and their interactions. Applications range from the use of hadroproduction processes to unveil nuclear structure and the behavior of quark and gluons at very high energies in proton-nucleus and nucleus-nucleus collisions [1], to the determination of, say, the quark and gluon polarization in polarized proton-proton and electron-proton collisions [2].

One cornerstone of these studies is the perturbative quantum chromodynamics (QCD) framework for single-inclusive high- p_T hadron production [3] and, more specifically, its description in terms of fragmentation functions (FFs), as they link the hard scattering of partons at short

distances to the hadrons observed in the final state [4]. Scale-dependent FFs factorize the relevant nonperturbative information on the hadronization process at long distances from the perturbative partonic cross sections and cancel consistently their final-state singularities [5].

Fifteen years ago, the first next-to-leading order (NLO) global QCD analysis of unidentified charged hadron FFs was presented in Ref. [6]. It combined data on single-inclusive electron-positron annihilation (SIA) with those from semi-inclusive deep-inelastic scattering (SIDIS) and proton-proton collisions (PP) and demonstrated the universality and factorization properties of FFs within the precision of the data at that time. Similar analyses were later published in [7–10] incorporating newer data and different theoretical refinements and analyses strategies.

Over the last decade, various LHC experiments [11–15] have produced remarkably precise hadroproduction data at increasing center-of-mass system (c.m. system) energies. One rather unexpected feature of these data is the sizable discrepancy with NLO predictions computed with FFs obtained previously from SIA, SIDIS, and PP data at lower c.m.s. energies. The tension aggravates to the point that it is not even possible to describe consistently datasets from the same LHC experiment if the c.m. system energies increases by a few TeV. This feature likely suggests a serious limitation of the NLO framework and has also been

^{*}ignacio.borsa@itp.uni-tuebingen.de

[†]marco.stratmann@uni-tuebingen.de

[‡]deflo@unsam.edu.ar

[§]sassot@df.uba.ar

Published by the American Physical Society under the terms of the Creative Commons Attribution 4.0 International license. Further distribution of this work must maintain attribution to the author(s) and the published article's title, journal citation, and DOI. Funded by SCOAP³.

observed in analyses of pion, kaon, and proton hadroproduction data [16].

Nevertheless, in Ref. [17], it has been demonstrated that the NLO QCD framework can still provide a rather accurate global description of data with identified pions up to the highest c.m. system energies available, and even down to p_T -values of around 1 GeV, if one fully exploits the factorization scale ambiguity that is inherent to any fixed-order perturbative QCD estimate. In doing so, one can hope to mimic the yet unknown higher order QCD corrections, in particular, their energy dependence. In the following, we show that this is also a viable path for analyzing data for other identified or unidentified final-state hadrons, including measurements in proton-antiproton collisions from the CDF experiment [18,19] and even the older UA1 and UA2 experiments at the CERN Super Proton Synchrotron [20,21]. Interestingly, the correlation between the most appropriate choice of factorization scale and the c.m. system energy is found to be the same as for pions in Ref. [17]. In this way, we are able to provide a new set of FFs for unidentified charged hadrons h^\pm that is suitable for up-to-date phenomenological applications at high energy hadron colliders.

We note that the new set of FFs is also constrained by very precise SIDIS data for unidentified charged hadrons from COMPASS [22] that were not available at the time when the analysis of Ref. [6] was presented. These results complement the pioneering measurements by EMC [23] that were employed previously. As is customary, the estimated residual uncertainties of the FFs are given in terms of a large set of replicas obtained by Monte Carlo sampling, which easily propagate to any observable, including the measurements used in the fit.

II. SETUP OF OUR GLOBAL ANALYSIS

Since the methodology we employ to extract the charged hadron FFs is identical to the one used for pions, we refer the reader to [17] and references therein for further details. In the following, we focus on the main features of the new datasets and the results of our analysis.

The aforementioned tension between the NLO estimates for hadroproduction cross sections and experimental results with increasing c.m. system energy \sqrt{s} , is best illustrated by the CMS [12,13] and ALICE [11,14] data, which are both included in our analysis. The data correspond to values of \sqrt{s} comprising 0.9, 2.76, and 7 TeV and a p_T range up to around 200 GeV. An advantage of comparing data from the same collaboration at different \sqrt{s} is to minimize potential discrepancies stemming from varying criteria used to identify and select certain final-state hadrons experimentally due to the underlying detector capabilities.

In Figs. 1 and 2, we compare CMS, ALICE, and PHENIX [24] data, all included in our global fit to be discussed below, against NLO estimates computed with

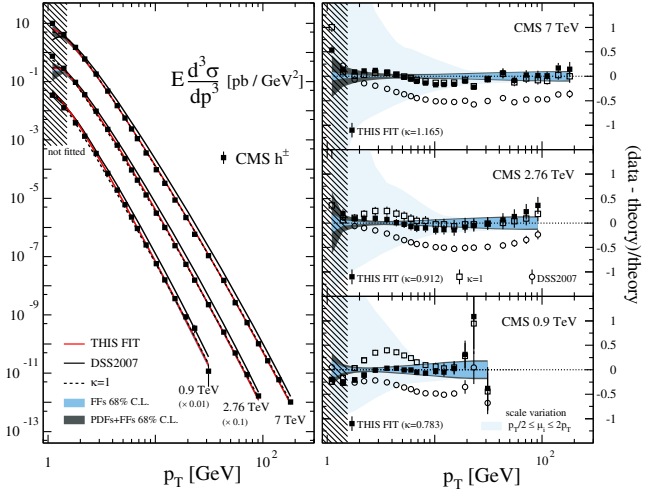


FIG. 1. lhs: Comparison of our best fit and other NLO results with the CMS data on h^\pm production [12,13] at different \sqrt{s} . rhs: “(data-theory)/theory” plots for each set of data. The relevant cuts and sources of uncertainties for our new fit are indicated by the shaded bands; see Sec. III below.

parton distribution functions (PDFs) from Ref. [25] and different choices of FFs. The estimates obtained with the pre-LHC set of FFs [6] are represented by solid black lines and open circles in the panels on left-hand-side (lhs) and right-hand-side (rhs) of both figures, respectively. Clearly, these results labeled as DSS2007 overestimate the CMS and ALICE data in the entire range of p_T shown in Figs. 1 and 2 but, at the same time, describe the PHENIX data at $\sqrt{s} = 200$ GeV, included in their fit, very well.

In addition, the LHCb experiment has recently reported measurements at $\sqrt{s} = 13$ TeV [15] that discriminate positively and negatively charged hadrons h^+ and h^- in various bins of (forward) rapidity η up to almost five units.

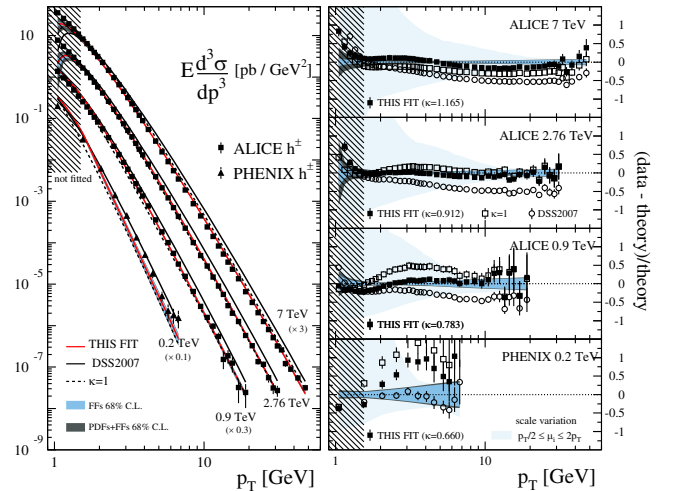


FIG. 2. As Fig. 1 but now for both ALICE [11,14] and PHENIX [24] data.

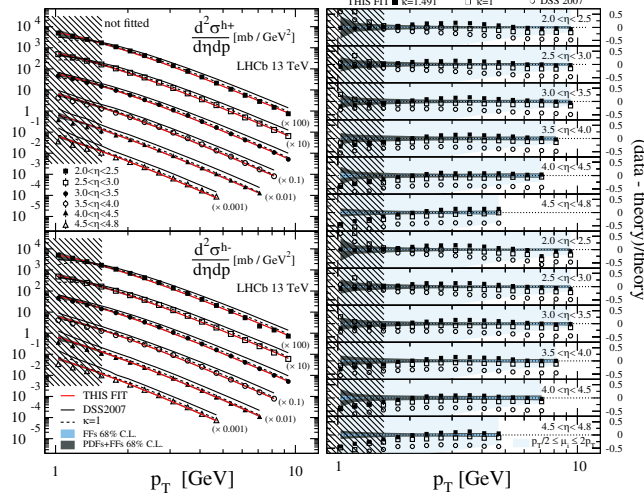


FIG. 3. As Fig. 1 but now for the charge separated h^+ and h^- data from LHCb [15] in different bins of rapidity.

These results nicely complement the charged averaged h^\pm ALICE and CMS data taken at central rapidities in our analysis. Again, the NLO estimates computed with the DSS2007 FFs [6] overestimate the data in the entire ranges of p_T and η explored by LHCb as can be inferred from Fig. 3.

In our fit, we include also charge-averaged h^\pm data taken in proton-antiproton collisions from both CDF and the UA1 and UA2 experiments, some of which are shown in Fig. 4. As before, the DSS2007 FFs tend to overestimate the data at larger \sqrt{s} , even though some of them were included in their analysis [6]. It is worth noticing that, at variance with the recent global analysis of pion FFs in Ref. [17], where the only source of conflicting high energy collider data stems from a single LHC experiment (ALICE), datasets from four experiments and from different colliders (LHC and Tevatron) show the same trend of NLO estimates

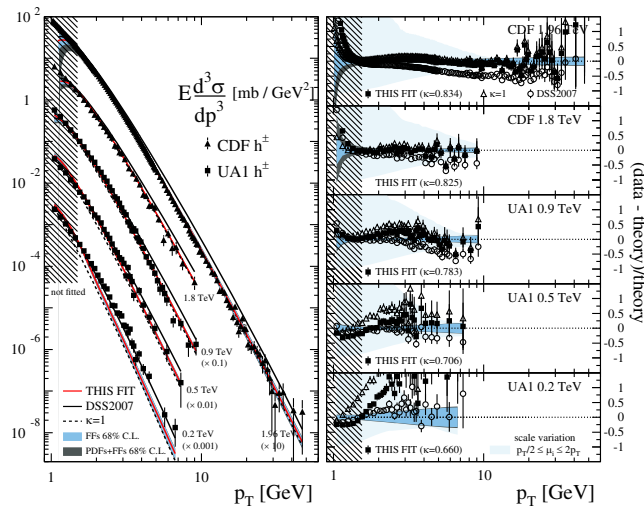


FIG. 4. As Fig. 1 but now for CDF [18,19] and UA1 [20] data.

grossly overshooting data in the case of unidentified charged hadrons h^\pm .

Along with the high- p_T hadroproduction results shown in Figs. 1–4, our new global QCD analysis of FFs for unidentified charged hadrons includes the same sets of SIA data [26–34] as in Ref. [6] as well as the SIDIS data on proton and deuteron targets from EMC [23]. A new, crucial asset in our fit are the much more precise SIDIS multiplicities for h^+ and h^- production from COMPASS [22], which are presented in a very detailed binning in the relevant kinematical variables. These data are instrumental to achieve the charge and flavor separation of the h^\pm FFs in our fit. In Fig. 5, we show a “(data-theory)/theory” comparison of the charge separated SIDIS multiplicities from COMPASS for various theoretical estimates. Contrary to the PP data in Figs. 1–4, the DSS2007 FFs [6] nicely reproduce the data. Again, the NLO estimates are computed with PDFs from Ref. [25] neglecting nuclear effects in the deuteron [35].

The present analysis of the h^\pm FFs differs in one important aspect from our previous fit in Ref. [6]. In the latter case, the h^\pm FFs were built up from the sum of the previously determined charged pion, kaon, and (anti)proton FFs plus a small residual component, which was actually fitted to the available data. Now we choose to parametrize the entire set of charged hadron FFs from scratch. The reasoning behind this is twofold. Firstly, the availability of many new and, most importantly, significantly more precise data allows us to constrain and fully discriminate

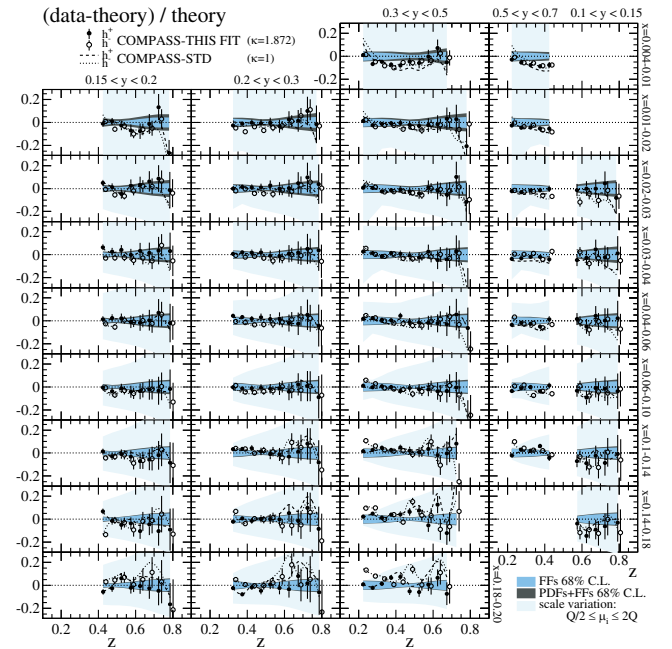


FIG. 5. “(Data-theory)/theory” comparisons of the DSS2007 and our best fit results to the charge separated h^+ and h^- SIDIS multiplicities from COMPASS. The shaded bands provide various uncertainty estimates; see Sec. III below.

between the flavors of the parton-to-charged hadron FFs in the fit. Secondly, it greatly facilitates the estimates of the remaining uncertainties of the obtained FFs by avoiding a cumbersome propagation and interplay of uncertainties stemming from pion, kaon, and (anti)proton FFs. Nevertheless, the fits obtained in either way are equally good, and the residual contribution to the newly obtained h^\pm FFs is indeed small and positive once the pion, kaon, and (anti)proton contributions are subtracted. In other words, the h^\pm FFs are consistent with the individual contributions of each of the identified hadron species contributing to the sum of unidentified charged hadron yields.

Finally, following the strategy of Ref. [17] for the extraction of pion FFs, we perform two fits that differ in the choice for the renormalization, initial-, and final-state factorization scale, μ_R , μ_{FI} , and μ_{FF} , respectively. In one fit, we adopt the standard choice; i.e., we set $\mu_R = \mu_{FI} = \mu_{FF} = \kappa\mathcal{E}$ with $\kappa = 1$ and \mathcal{E} being the typical hard scale of the process under consideration (e.g., p_T in PP). In our best fit, which gives a much better global description of the datasets entering the analysis, we treat κ as free parameter for each experiment or group of experiments with similar kinematics. It turns out that the κ values that have been obtained in the analysis of pion FFs [17] also lead to a very close to optimum description of the charged hadron data. Therefore, we simply adopt the κ values from the pion fit rather than refitting them. A similar observation can be made for fits of charged kaon and (anti)proton FFs, which will be reported elsewhere. We also replicate the strategy of Ref. [17] for the estimation of the uncertainties of the resulting set of FFs. Using the optimum values of the fit parameters κ , and through the application of a Monte Carlo sampling technique, we generate an ensemble of $N_{\text{rep}} = 500$ replicas of the FFs. The uncertainty stemming from the FFs in any observable is then assumed to be given statistically by the standard deviation of the observable calculated over the set of replicas.

III. DISCUSSION OF THE FIT RESULTS

The hadroproduction cross section estimates computed with our new optimum set of charged hadron FFs, i.e., obtained from the fit by adopting the scale factors κ from the pion fit [17], are shown as red solid lines on the lhs of Figs. 1–4, and by filled rectangles in the corresponding “(data-theory)/theory” plots on the rhs of each figure. The alternative results calculated with the standard choice $\kappa = 1$ are represented by dashed lines and open rectangles, respectively. In addition to the NLO estimates, Figs. 1–4 also present the uncertainty bands associated with the nonperturbative inputs of the calculations at the 68% confidence level (CL), i.e., from the used sets of FFs and PDFs (blue and gray shaded bands), as well as the theoretical uncertainty stemming from the truncation of the perturbative series (light blue shaded bands). The latter is estimated

performing the so-called 27-point independent variation of the renormalization and factorization scales in the range $p_T/2 \leq \mu \leq 2p_T$.

Notice that FFs uncertainty bands are in most cases hardly visible in the left-hand side panels of Figs. 1–4 because of the range of values spanned by the proton-proton hadroproduction cross section. Nevertheless, they are plotted in the right-hand side panels of those figures as a relative error.

In contrast to the analysis of Ref. [6], the fit to the PP data set is now primarily driven by the very precise measurements taken at higher c.m. system energies of the LHC. As can be seen, the $\kappa = 1$ fit reproduces fairly well the data at energies of around $\sqrt{s} = 7$ and 13 TeV, while the quality of the fit degrades sharply towards smaller values of \sqrt{s} . The use of the scale variable κ , on the other hand, mitigates some of the tension leading to a nice description of hadroproduction data from the highest c.m. system energies down to $\sqrt{s} \simeq 0.5$ TeV and significantly improves the agreement with data at $\sqrt{s} \simeq 0.2$ TeV as compared to the $\kappa = 1$ results. In the latter case, the DSS2007 fit still provides the best results but, as previously mentioned, grossly overestimates all LHC data.

We note that for SIA and SIDIS, the agreement of data with the theoretical estimates is to a much lesser extent affected by the choice of scales than calculations for PP. In the SIDIS multiplicities, the dependence on the scales μ_R , μ_{FI} , and μ_{FF} tends to cancel in the relevant ratios of the semi-inclusive and the inclusive cross section. For completeness, the optimum values of κ for each set of data are indicated in Figs. 1–5.

In Fig. 6, we compare the newly obtained optimum set of FFs $zD_i^{h^+}(z, Q^2)$ for positively charged hadrons, multiplied by the momentum fraction z , at a scale $Q = 10$ GeV for all parton flavors i to the previous analysis by DSS. The shaded band indicates our estimates for the uncertainties of the FFs for each flavor at the 68% confidence level.

As can be seen, there are sizable differences between the current and the DSS results [6] for all light quark flavor combinations $q + \bar{q}$, where $q = u, d, s$. In case of $u + \bar{u}$, they originate largely from the unfavored flavor \bar{u} , where favored and unfavored refer to the valence content of a π^+ meson. The fragmentation into a π^+ contributes by far the most to the sum of FFs into a positively charged hadron h^+ . Likewise, we find that for $d + \bar{d}$, the differences for the favored contribution from \bar{d} are much more moderate than for the unfavored d . We recall that the flavor separation in the DSS2007 extraction [6] was mainly driven by the EMC SIDIS data [23], and, to some extent, by preliminary Hermes results used to constrain pion and kaon FFs [36]. In the current fit, the separation of the h^\pm FFs into different parton flavors comes mostly from the much more precise COMPASS data [22] shown in Fig. 5. It should be kept in mind though that SIDIS data are only available for hadron momentum fractions $z \geq 0.2$.

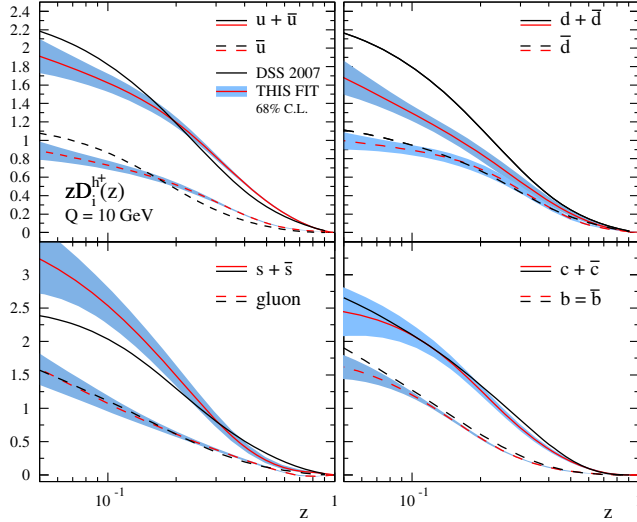


FIG. 6. The obtained optimum FFs (red lines) for positively charged hadrons for all parton flavors at scale $Q = 10$ GeV along with uncertainty estimates at 68% CL and compared to the previous results (black lines) from DSS2007 [6].

Hence, for smaller values of z , the flavor separation is at best an extrapolation driven by constraints at higher z .

On the other hand, the best experimental information on heavy flavor FFs still stems from flavor-tagged SIA data. So, it is not surprising that the differences for charm and bottom FFs, shown in the lower right panel of Fig. 6, are very small. What comes as a surprise is the similarity between the gluon FF in both fits. In the DSS2007 analysis, the gluon FF followed from a compromise between UA1/UA2 and the Tevatron data, while the current fit makes use of a wealth of LHC hadroproduction data. We therefore conclude that the observed similarity is most likely purely accidental.

Finally, in Table I, we summarize the datasets used in the current NLO global QCD analysis, the computed normalization shifts N_i as defined in Eq. (6) of Ref. [37], and the corresponding partial χ^2 values. As in all previous fits [6,17,37], we include only SIA data for hadron momentum fractions $z > 0.1$ since the hadrons are treated as massless in the factorized QCD framework. All the contributing datasets from SIA are very well reproduced with the possible exception of the light quark flavor-tagged data from DELPHI. As was mentioned above, SIDIS data are only available for $z > 0.2$. It turns out that the very precise, new COMPASS data are remarkably well reproduced by the fit, while the old EMC data for negatively charged hadrons have a rather large partial χ^2 and also acquire large normalization shifts. However, most of the large χ^2 contribution stems from just a few data points. Hadroproduction data taken in proton-(anti)proton collisions give the largest contribution to the total χ^2 of the fit. Here, we adopt a cut $p_T > 1.5$ GeV in the transverse momentum of the detected charged hadron for all datasets

TABLE I. Datasets, normalizations N_i as defined in Eq. (6) of [37], and the partial and total χ^2 values obtained in the fit.

Experiment	Data type	Relative normalization in fit	Data fitted	χ^2
TPC [26]	Inclusive	0.983	17	11.6
SLD [27]	Inclusive	1.026	21	18.0
ALEPH [28]	Inclusive	1.028	27	19.6
DELPHI [29]	Inclusive	1.048	12	8.3
	“ <i>uds</i> tag”	1.048	12	15.0
	“ <i>b</i> tag”	1.048	12	2.1
TASSO [31]	Inclusive (44 GeV)	1.035	14	10.5
	Inclusive (35 GeV)	1.035	14	15.9
OPAL [32]	Inclusive	1.057	12	6.5
	“ <i>uds</i> tag”	1.057	12	10.4
	“ <i>c</i> tag”	1.057	12	6.4
	“ <i>b</i> tag”	1.057	12	3.5
ALEPH [28]	Inclusive longitudinal	1.028	11	2.5
OPAL [33]	Inclusive longitudinal	1.057	12	3.0
DELPHI [34]	Inclusive longitudinal	1.048	12	13.2
	“ <i>uds</i> tag long.”	1.048	12	38.6
	“ <i>b</i> tag long.”	1.048	12	5.0
<i>SIA data</i>			236	190.1
EMC [23]	$p - h^+$	1.28	108	102.9
	$p - h^-$	1.28	108	223.3
	$d - h^+$	1.45	116	118.3
	$d - h^-$	1.45	116	239.9
COMPASS [22]	$d - h^+$	0.989	311	179.4
	$d - h^-$	0.989	311	129.1
<i>SIDIS data</i>			1070	992.9
PHENIX [24]	0.20 TeV	1.066	11	90.2
UA1 [20]	0.20 TeV	1.451	27	121.6
	0.50 TeV	1.068	27	30.5
	0.63 TeV	1.592	38	142.5
	0.90 TeV	1.094	35	45.5
UA2 [21]	0.54 TeV	0.975	27	70.9
CDF [18]	0.63 TeV	0.777	38	15.1
[18]	1.80 TeV	1.974	32	41.2
[19]	1.96 TeV	1.010	145	219.1
CMS [12]	0.90 TeV	0.947	15	38.7
[13]	2.76 TeV	0.999	19	23.6
[12]	7.00 TeV	0.948	22	91.7
ALICE [14]	0.90 TeV	0.981	32	69.3
[14]	2.76 TeV	0.954	37	23.1
[11]	7.00 TeV	0.948	43	92.3
LHCb [15]	13.0 TeV	1.034	140	775.5
<i>PP data</i>			688	1890.8
<i>TOTAL:</i>			1994	3073.8

except for LHCb, where we require $p_T > 1.56$ GeV to limit unwanted uncertainties from the PDFs, propagating into the cross section calculations, to a reasonable level.

While the overall description of the PP data is good and much improved as compared to calculations based on the DSS2007 set of charged hadron FFs, it is certainly not perfect. Some older sets from UA1 and CDF receive large normalization shifts, which is most likely an indication that these data lead to unresolvable tensions when combined with other measurements, similarly for the EMC SIDIS data for negatively charged hadrons. The LHC data, which span a large energy and p_T range and, in case of LHCb, also a fairly extreme kinematical coverage in terms of rapidity, are all remarkably well reproduced in the fit along with other probes from SIA and SIDIS. It should be also kept in mind that the scale uncertainties for the PP cross section estimates at NLO accuracy are extremely large below $p_T \simeq 5$ GeV as can be seen in the panels on rhs of Figs. 1–3.

IV. SUMMARY AND CONCLUSIONS

We have presented an updated set of parton-to-unidentified charged hadron fragmentation functions at NLO accuracy. It reproduces the latest LHC hadroproduction data at different c.m. system energies and down to transverse momentum values of about 1.5 GeV in a global analysis together with results from SIA, SIDIS, and older hadroproduction data taken in proton-(anti)proton collisions at various energies. As in the recent analysis of pion FFs in Ref. [17], the best fit exploits the freedom in the choice of the renormalization and factorization scales. In addition, a second set of FFs with conventional factorization and renormalization scale choices is provided.

The new analysis supersedes the extraction of FFs presented in Ref. [6] in many ways. Firstly, because of the inclusion of the latest experimental information from the LHC and the COMPASS SIDIS data, and, secondly, in the way uncertainties are estimated and presented through Monte Carlo replicas. The latter allow one to easily propagate the obtained uncertainties of the charged hadron FFs to any observable depending on them.

The significance of the factorization scale dependence and the need to utilize it in the fit points to a limitation of the NLO approximation, which is much more pronounced in proton-(anti)proton collisions than in the other processes studied. Interestingly and reassuringly, the scale choices that optimize the unidentified charged hadron FFs in our fit are indistinguishable from those found for pions in another recent global analysis. This is to be expected as charged hadrons produced in hard proton-(anti)proton collisions are dominated by pions.

We believe that the current NLO analysis provides a useful and up-to-date tool for phenomenological studies involving charged hadron FFs. These include not only hadroproduction in proton-proton and proton-nuclei collisions, but also SIDIS measurements at the future Electron Ion Collider [38] and as a way to further constrain PDFs at the comparatively lower energy scales typical of SIDIS experiments [39]. Despite its shortcomings in describing the energy dependence of currently available PP data in all its details, it accurately reproduces the main features of the different probes adopted in the global analysis. A better understanding of single-inclusive hadroproduction cross sections can be only expected once the full QCD corrections at next-to-next-to-leading order accuracy become available. Then it remains to be seen whether the theoretical description and the scale dependence will improve or if the underlying framework has some serious shortcomings such as significant factorization breaking effects.

ACKNOWLEDGMENTS

This work was supported in part by CONICET, ANPCyT, UBACyT, the Bundesministerium für Bildung und Forschung (BMBF), Grant No. 05P21VTCAA, and the Deutsche Forschungsgemeinschaft (DFG) through the Research Unit FOR 2926 (Project No. 40824754).

-
- [1] M. Klasen and H. Paukkunen, [arXiv:2311.00450](https://arxiv.org/abs/2311.00450).
 - [2] I. Borsa, G. Lucero, R. Sassot, E. C. Aschenauer, and A. S. Nunes, *Phys. Rev. D* **102**, 094018 (2020).
 - [3] J. C. Collins, D. E. Soper, and G. F. Sterman, *Adv. Ser. Dir. High Energy Phys.* **5**, 1 (1989).
 - [4] R. D. Field and R. P. Feynman, *Phys. Rev. D* **15**, 2590 (1977).
 - [5] J. C. Collins and D. E. Soper, *Nucl. Phys.* **B194**, 445 (1982).
 - [6] D. de Florian, R. Sassot, and M. Stratmann, *Phys. Rev. D* **76**, 074033 (2007).
 - [7] V. Bertone, N. P. Hartland, E. R. Nocera, J. Rojo, and L. Rottoli (NNPDF Collaboration), *Eur. Phys. J. C* **78**, 651 (2018).
 - [8] A. Mohamaditabar, F. Taghavi-Shahri, H. Khanpour, and M. Soleymaninia, *Eur. Phys. J. A* **55**, 185 (2019).
 - [9] M. Soleymaninia, M. Goharipour, H. Khanpour, and H. Spiesberger, *Phys. Rev. D* **103**, 054045 (2021).
 - [10] E. Moffat, W. Melnitchouk, T. C. Rogers, and N. Sato (Jefferson Lab Angular Momentum (JAM) Collaboration), *Phys. Rev. D* **104**, 016015 (2021).
 - [11] K. Aamodt *et al.* (ALICE Collaboration), *Eur. Phys. J. C* **68**, 345 (2010).
 - [12] S. Chatrchyan *et al.* (CMS Collaboration), *J. High Energy Phys.* **08** (2011) 086.
 - [13] S. Chatrchyan *et al.* (CMS Collaboration), *Eur. Phys. J. C* **72**, 1945 (2012).

- [14] B. B. Abelev *et al.* (ALICE Collaboration), *Eur. Phys. J. C* **73**, 2662 (2013).
- [15] R. Aaij *et al.* (LHCb Collaboration), *J. High Energy Phys.* **01** (2022) 166.
- [16] D. d'Enterria, K. J. Eskola, I. Helenius, and H. Paukkunen, *Nucl. Phys.* **B883**, 615 (2014).
- [17] I. Borsa, R. Sassot, D. de Florian, and M. Stratmann, *Phys. Rev. D* **105**, L031502 (2022).
- [18] F. Abe *et al.* (CDF Collaboration), *Phys. Rev. Lett.* **61**, 1819 (1988).
- [19] T. Aaltonen *et al.* (CDF Collaboration), *Phys. Rev. D* **79**, 112005 (2009).
- [20] C. Albajar *et al.* (UA1 Collaboration), *Nucl. Phys.* **B335**, 261 (1990).
- [21] M. Banner *et al.* (UA2 and Bern-CERN-Copenhagen-Orsay-Pavia-Saclay Collaboration), *Z. Phys. C* **27**, 329 (1985).
- [22] C. Adolph *et al.* (COMPASS Collaboration), *Phys. Lett. B* **764**, 1 (2017).
- [23] J. Ashman *et al.* (European Muon Collaboration), *Z. Phys. C* **52**, 361 (1991).
- [24] S. S. Adler *et al.* (PHENIX Collaboration), *Phys. Rev. Lett.* **95**, 202001 (2005).
- [25] S. Bailey, T. Cridge, L. A. Harland-Lang, A. D. Martin, and R. S. Thorne, *Eur. Phys. J. C* **81**, 341 (2021).
- [26] H. Aihara *et al.* (TPC Collaboration), *Phys. Rev. Lett.* **61**, 1263 (1988); *Phys. Lett. B* **184**, 299 (1987); X.-Q. Lu, Ph.D. thesis, Johns Hopkins University Report No. UMI-87-07273, 1986.
- [27] K. Abe *et al.* (SLD Collaboration), *Phys. Rev. D* **59**, 052001 (1999).
- [28] D. Buskulic *et al.* (ALEPH Collaboration), *Z. Phys. C* **66**, 355 (1995); *Phys. Lett. B* **357**, 487 (1995); R. Barate *et al.* (ALEPH Collaboration), *Phys. Rep.* **294**, 1 (1998).
- [29] P. Abreu *et al.* (DELPHI Collaboration), *Eur. Phys. J. C* **5**, 585 (1998).
- [30] G. Abbiendi *et al.* (OPAL Collaboration), *Eur. Phys. J. C* **16**, 407 (2000).
- [31] W. Braunschweig *et al.* (TASSO Collaboration), *Z. Phys. C* **42**, 189 (1989).
- [32] K. Ackerstaff *et al.* (OPAL Collaboration), *Eur. Phys. J. C* **7**, 369 (1999).
- [33] R. Akers *et al.* (OPAL Collaboration), *Z. Phys. C* **68**, 203 (1995).
- [34] P. Abreu *et al.* (DELPHI Collaboration), *Eur. Phys. J. C* **6**, 19 (1999).
- [35] L. N. Epele, H. Fanchiotti, C. A. Garcia Canal, and R. Sassot, *Phys. Lett. B* **275**, 155 (1992).
- [36] D. de Florian, R. Sassot, and M. Stratmann, *Phys. Rev. D* **75**, 114010 (2007).
- [37] D. de Florian, R. Sassot, M. Epele, R. J. Hernández-Pinto, and M. Stratmann, *Phys. Rev. D* **91**, 014035 (2015).
- [38] E. C. Aschenauer, I. Borsa, R. Sassot, and C. Van Hulse, *Phys. Rev. D* **99**, 094004 (2019).
- [39] I. Borsa, R. Sassot, and M. Stratmann, *Phys. Rev. D* **96**, 094020 (2017).